N-doped graphene quantum dots-functionalized titanium dioxide nanofibers and their highly efficient photocurrent response

Xiaotian Wang, Dandan Ling, Yueming Wang, Huan Long, Yibai Sun,[a] Yanqiong Shi, Yuchao Chen, Yao Jing, Yueming Sun, and Yunqian Dai[b]
School of Chemistry and Chemical Engineering, Southeast University, Nanjing, Jiangsu 211189, People's Republic of China

(Received 6 March 2014; accepted 18 June 2014)

Titanium dioxide (TiO_2), a widely used inorganic semiconductor owing to its superb photoelectric properties, has frequently been fabricated into composites to reduce its relatively large band gap and overcome its limited visible light absorption. In this article, a "layer-by-layer" method has been developed to prepare the composite structure of nitrogen (N)-doped graphene quantum dots (GQDs)-sensitized TiO_2 nanofibers. The as-prepared structure shows considerable luminescence and exhibits excellent photoelectric properties. Various factors including the crystalline phase of TiO_2, amount of N in GQDs, and irradiation wavelength were investigated to find the optimal conditions for enhanced photoelectric activity. It is demonstrated that the combination of highest N amount GQDs with TiO_2 nanofibers of mixed phases (750 °C-sintered TiO_2 nanofibers) possess the best photoelectric properties. The enhancement of properties using TiO_2 nanofibers with mixed phases mainly contributes to the transfer of electrons between conduction bands of different phases in TiO_2 and the distinctive photoluminescence (PL) property of N-GQDs. Furthermore, this enhancement can be achieved in most areas of the visible light range. The general mechanism of the electron generation and transfer of the structure is based on the normal PL and upconversion PL property of N-GQDs which serve as the sensitizer. We consider it a feasible method to improve the photoelectric conversion efficiency in photovoltaic devices.

I. INTRODUCTION

Graphene quantum dots (GQDs), a novel type of graphene materials, have aroused enormous interest due to their excellent chemical and physical properties.[1–4] On top of unique electron transportation properties[5] inherited from graphene, GQDs share with carbon dots advantages such as chemical inertness, low cytotoxicity, and excellent biocompatibility. Beyond that, GQDs possess a novel phenomenon which is related to quantum confinement and edge effects.[6,7] These distinctive properties lead to their various applications in photovoltaics.[2,8] Substitutional N-doping of graphitic carbon materials has proved to be an effective method to modify their electronic properties and chemical reactivity for their extensive application in numerous fields, such as lithium batteries,[9] ultracapacitors,[10] electrocatalysis,[11] and hydrogen storage.[12] Therefore, doping GQDs with nitrogen opens up new prospects for the utilization of GQDs as a consequence of the drastic modification of their electronic properties and creation new active sites.[4] Li et al.[13] synthesized N-doped GQDs by hydrothermal approach and studied their distinctive photoluminescence (PL) properties, which are different from those of N-free GQDs. Several reports applied N-GQDs in oxygen reduction reaction and they exhibit superior electrocatalytic ability.[11,14]

Titanium dioxide (TiO_2) is a superb inorganic semiconductor due to its desirable electronic and optical properties combined with low cost, low toxicity, and high physical and chemical stability. Nanostructured TiO_2 such as nanofibers, nanowires, nanocrystals, and nanotubes has presented exceptional physical and chemical qualities over their bulk counterparts owing to dimension-dependent properties.[15] 1D TiO_2 nanofibers, especially, have stimulated tremendous breakthroughs in the field of sensing, photovoltaics, and photocatalysis due to their intriguing electronic and optical properties. As a wide-band gap semiconductor with about 3.2 and 3.0 eV for anatase and rutile respectively, however, TiO_2 can only absorb light in ultraviolet region which severely limits their photovoltaic and photocatalytic applications. Thus, a common way to solve this problem is attempting to narrow the band gap of semiconducting TiO_2 to improve absorption in the visible region to harvest light with longer wavelengths for higher photovoltaic and photocatalytic activity. An effective method is to make a composite structure of TiO_2 with carbon-containing materials, such as conjugated polymers and molecular chromophores. The superb properties of nanoscale graphitic carbon materials lead to increasing

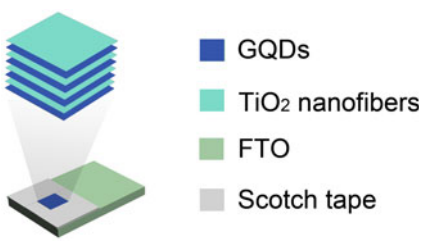
Address all correspondence to these authors.
[a]email: Sun@seu.edu.cn
[b]email: Daiy@seu.edu.cn
DOI: 10.1557/jmr.2014.152

 © Materials Research Society 2014

https://doi.org/10.1557/jmr.2014.152 Published online by Cambridge University Press

interest in their application in composite structure with TiO_2. Long et al.[16] synthesized graphene–TiO_2 composites and penetratingly investigated their electronic structure and mechanisms of photoinduced charge separation process across the graphene–TiO_2 interface. However, previous work[17,18] indicates that both graphene oxide (GO)/TiO_2 and reduced graphene oxide (RGO)/TiO_2 composites can only improve photoelectrical property of TiO_2 under the irradiation of wavelength longer than 510 nm. Moreover, Zhuo and coworkers[3] prepared a GQDs/TiO_2 complex system which harnessed the visible spectrum of sunlight for the use of high-efficiency photocatalyst. All three works detected the photocurrent response of the composite material but the values were relatively low which indicates limited enhancement of their photoelectrical property.

Previous work in our group[19] described a facile method to engineer the interfacial coupling between reduced graphene oxide (RGO) and TiO_2 in well-designed 1D RGO-wrapped TiO_2 nanofibers, which act as ultrafast electron transfer bridges when implanted in photoanodes. Remarkably enhanced photoelectric property was observed due to interfacial charge transfer. Herein, we utilized N-doped GQDs to sensitize TiO_2 nanofibers by a so-called "layer-by-layer" method for high photoelectrical performance, the structure of which is illustrated in Scheme 1. For comparison, a similar method was also used to synthesize N-free GQDs-sensitized TiO_2 nanofibers. One of the highlights of this work is that nanostructured materials were extensively used within the experiments to leverage their various advantages mentioned above. The Shockley–Queisser limit[20] indicates that to efficiently convert captured photons into photocurrent, the energy of the photons should exceed the energy gap of the sensitizer (GQDs) and the so-called "hot electrons" (photoexcited electrons) should be captured before they recombine. Williams and coworkers[21] found that time constant of electron injection from photoexcited GQDs to the conduction band of TiO_2 is less than 15 femtosecond (fs) and the time constant of electron-hole recombination is higher than 80 fs, which means hot electrons can be successfully captured in GQDs/TiO_2 composite system. Therefore, we can narrow our focus to effectively exciting electrons in GQDs-sensitized TiO_2 nanofibers. In this work, the influences of TiO_2's crystalline phase, the types of GQDs, and the irradiation wavelength on photoelectrical properties were systematically investigated and the composite structure was found to behave well in generating photocurrent. We expect that our achievement may motivate the photovoltaic and photocatalytic application of these materials.



SCHEME 1. Schematic of the ultimate product of the device containing GQDs-sensitized TiO_2 nanofibers.

II. EXPERIMENTAL SECTION

A. Chemicals

Graphite powder (99.95%, 325 mesh) and ethanol (97%) were purchased from Alfa Aesar (Ward Hill, MA). Titanium tetraisopropoxide (TTIP, 97%), Nafion (10 wt%, water solution), and poly(vinyl pyrrolidone) (PVP, $M_w \approx 1{,}300{,}000$) were obtained from Sigma. Other agents were purchased from Sinopharm Group Co. Ltd. (China) Ultrapure water (18.5 MΩ cm^{-1}) was used throughout the experiments.

B. Preparation of TiO_2 nanofibers and GQDs

TiO_2 nanofibers were electrospun according to the method described in our previous work.[22] Typically, 0.3 g of PVP was completely dissolved in 4.5 mL of ethanol followed by the addition of 2.5 mL of TTIP and 3.0 mL of acetic acid. A voltage of 16.5 kV was imposed and the solution was pumped at a controlled rate of 0.3 mL/h. The as-prepared TiO_2 nanofibers were sintered in air at 510, 750, and 950 °C for 4.5 h respectively to form desired crystalline phases.

GQDs were also prepared and characterized following protocol previously utilized in our group.[23] Briefly, graphene oxide (GO) sheets were fabricated from graphite by a modified Hummers method.[24] Then, 20 mg of GO sheets was sonicated for 1 h followed by the addition of 0, 5, 10, 15, and 20 mL of ammonia respectively and the final products of GQDs were denoted from GQDs-1 to GQDs-5 accordingly. The suspension was removed to a poly(tetrafluoroethylene) (Teflon)-lined autoclave and heated at 200 °C for 8 h. The obtained black suspension was centrifuged at 15,000 rpm for 10 min to obtain supernatant brown liquids. To suspend the GQDs in ethanol, water was removed by rotary evaporation and the appropriate amount of ethanol was added to achieve the desired concentration of GQDs.

C. Fabrication of the photoanodes based on GQDs-sensitized TiO_2 nanofibers

The composite structure of GQDs-sensitized TiO_2 nanofibers was achieved by a so-called "layer-by-layer" method on the surface of fluorine-doped tin oxide (FTO) photoanodes. Typically, the TiO_2 nanofibers were dispersed in ethanol to make 5 mg/mL suspension by ultrasonication for 2 h. GQDs-sensitized TiO_2 photoanodes were fabricated by alternately dropping 2.5 μL of ethanol suspension of TiO_2 nanofibers and 2.5 μL of GQDs suspended in ethanol eight

https://doi.org/10.1557/jmr.2014.152 Published online by Cambridge University Press

times onto a given 5 mm × 5 mm area of FTO, followed by dropping 5 μL of nafion (0.1 wt%, ethanol solution) to protect electrode materials from exfoliating in electrolyte. The whole structure of the device is illustrated in Scheme 1.

D. Measurements of photocurrent response

GQDs-sensitized TiO_2 nanofibers were measured in a three-electrode system consisting of a GQDs-TiO_2/FTO working electrode, a platinum wire auxiliary electrode, and an Ag/AgCl (3 M KCl) reference electrode which were immersed in 10 mM $NaNO_3$ solution as the electrolyte. The three-electrode testing system was irradiated by a Xe lamp (CEL-HXF300/CEL-HXUV300, education Au-light Co., Beijing, China) equipped with filters of different wavelengths. The photocurrent response was recorded by a CHI 760B electrochemical workstation (CH Instrument, Chenhua Co., Shanghai, China) with an initial imposed voltage of 0.2 V.

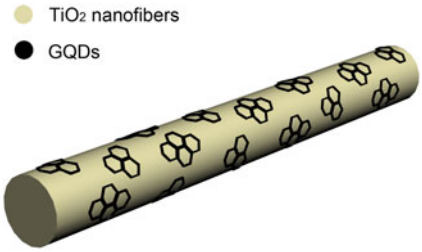
E. Characterizations

X-ray diffraction (XRD) pattern was carried out by a Bruker D8 Advanced diffractometer (Billerica, MA) using Cu K_α (1.5406 Å) radiation. Raman spectra were tested using a Thermo Fisher Scientific DXR Raman Microscope (Waltham, MA) with a 532 nm laser beam. The fluorescent images were taken using Fluorescence Microscopy (Olympus BX53).

III. RESULTS AND DISCUSSION

TiO_2 nanofibers were prepared by electrospinning and sintered at different temperatures to remove organic residues and achieve the desired crystalline phase. The evolution of their crystal structure was characterized by Raman spectrum (Fig. S1) in which the content of rutile phase increased with the augmentation of sintering temperature. XRD pattern (Fig. S2) of the sintered TiO_2 fibers quantified the temperature-dependence of the crystal structure: 100 wt% anatase at 510 °C, 35.97 wt% anatase versus 64.03 wt% rutile at 750 °C, and 100 wt% rutile at 950 °C. Fluorescent microscopy images of TiO_2 nanofibers (750 °C) (Fig. S3) indicate that there is almost no fluorescent light under bridged nucleic acid (BNA) and glycol nucleic acid (GNA) irradiation despite some dim scattered light under UW irradiation due to the nanoscaled structure of TiO_2 nanofibers. Previous studies[25,26] demonstrate that unlike bulk and single crystal TiO_2, nanostructured TiO_2 possesses some PL, the intensity of which grows with the diminution of nanostructures' size. This phenomenon was attributed to numerous surface states within the forbidden gap of TiO_2 which are generated by impurities and defects. The images of GQDs-sensitized TiO_2 nanofibers (750 °C) (Fig. S3), however, show a tremendous fluorescent light enhancement after adding GQDs, indicating the successful sensitization of GQDs on TiO_2 nanofibers. The particles of GQDs are assumed to be attached on the surface of TiO_2 nanofibers which is illustrated in Scheme 2. Similar results are found in 950 °C-sintered TiO_2 nanofibers (Fig. S4).

Raman spectroscopy is a common method to characterize the intrinsic structure of TiO_2/graphite material composites such as TiO_2/RGO[27,28] and TiO_2/GO.[29] Therefore, we used Raman spectra (Fig. 1) of GQDs-sensitized TiO_2 nanofibers (750 °C) to further verify their composite structure. The frequencies of ~144 cm^{-1}, ~319 cm^{-1}, and 517 cm^{-1}(labeled 1, 3, and 5) are ascribed to the structure of anatase TiO_2 while those of ~238 cm^{-1}, ~446 cm^{-1}, and ~611 cm^{-1} are corresponded to the structure of rutile TiO_2 in addition to the D and G[28,30] band at ~1355 cm^{-1} and ~1585 cm^{-1}. The data suggest the successful fabrication of GQDs-sensitized TiO_2 nanofibers (750 °C). The intensity ratios of the D band to that of anatase TiO_2 at ~144 cm^{-1} are around 0.25, 0.33, 0.34, 0.5, and 1.09 from GQDs-1-sensitized TiO_2 nanofibers to GQDs-5-sensitized TiO_2 nanofibers, which is corresponded with the results in UV-vis spectrum (Fig. S5). Because TiO_2 nanofibers were sensitized by different GQDs suspension with same volume in Raman tests, those results could be used to evaluate the concentration of GQDs in the ethanol suspension, the value of which could later be normalized accordingly to maintain the extent of sensitization within all types of GQDs/TiO_2 composite structure. Various studies have proved that the D band is related to edges, defects, and dangling bonds while the G band is ascribed to ordered sp^2-bonded carbon atoms. The intensity ratios of the D band to the G band, therefore, are always treated as a significant measure of disorder in graphitic materials: the higher the I_D/I_G value, the higher the defect concentration.[27] In this work, the values of I_D/I_G are around 0.77, 0.96, 1.06, 1.02, and 1.01 from GQDs-1-sensitized TiO_2 nanofibers to GQDs-5-sensitized TiO_2 nanofibers. Apparently, the addition of ammonia leads to defects which are brought about by lattice substitution of N in the π-conjugated system within the structure of GQDs. Further addition of ammonia fails to exacerbate the defects, possibly due to a "defect-repair" process which inhibits the emergence of new defects and keeps I_D/I_G value constant.[28] Similar results are achieved (Fig. S6) in GQDs-sensitized TiO_2 nanofibers (950 °C)



SCHEME 2. Schemetic of the microstructure of GQDs-sensitized TiO_2 nanofibers.

https://doi.org/10.1557/jmr.2014.152 Published online by Cambridge University Press

despite the disappearance of peaks at ~319 cm^{-1} and 517 cm^{-1} and substantial decrease of the peak at ~144 cm^{-1}, which is consistent with the result of crystal morphology ratio in XRD spectrum showing that the anatase phase has been completely eliminated after calcination at 950 °C.

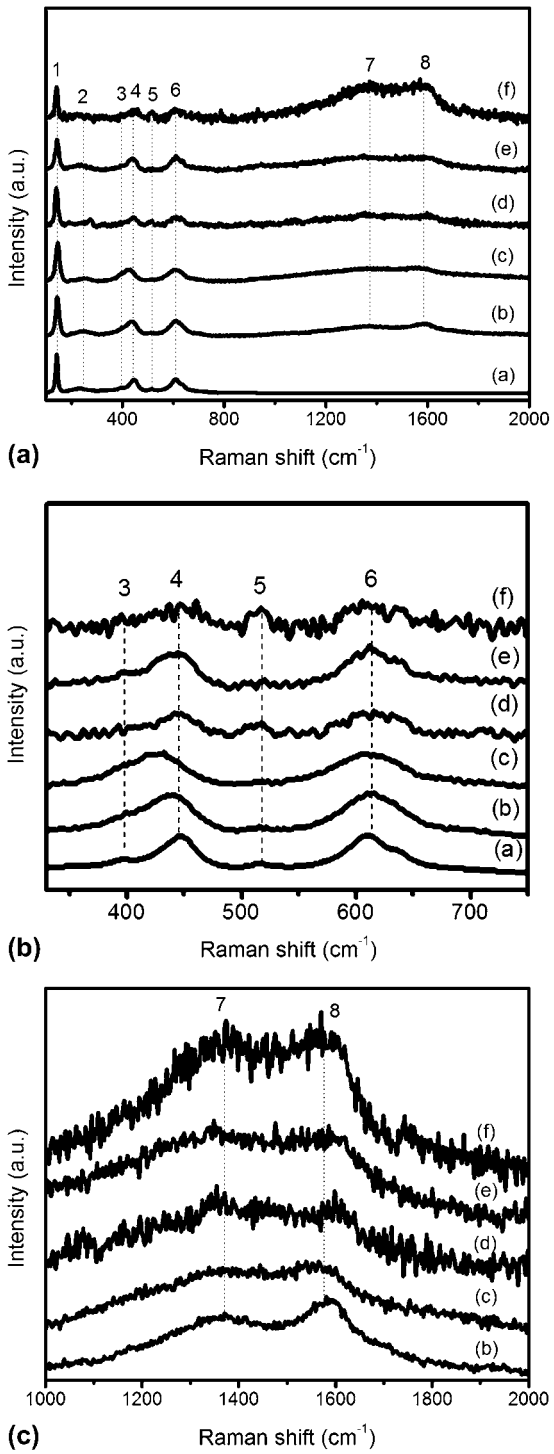
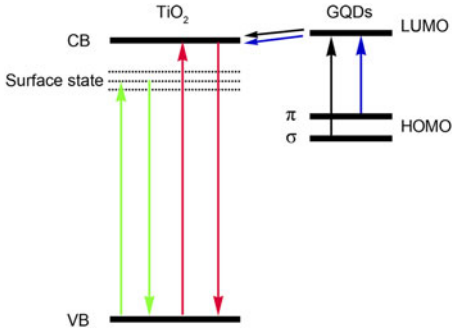


FIG. 1. Raman spectra of (a) TiO_2 nanofibers (750 °C) and (b)–(f) GQDs-1-sensitized TiO_2 nanofibers (750 °C) to GQDs-5-sensitized TiO_2 nanofibers (750 °C). A is the original image while B and C present details of specific peaks.

Reproducible photocurrent response to ON–OFF light cycles on the GQDs-sensitized TiO_2 photoanodes was tested in the three-electrode system to characterize their photoelectrical properties. The effect of TiO_2 crystalline phase is first investigated to determine a proper backbone for the electrode under the irradiation of visible light with a 420 nm cutoff filter. The photoelectric properties of TiO_2 with different crystalline phases have long been studied. According to literature work,[31] rutile TiO_2 exhibits higher photoelectrical activity than anatase TiO_2 under visible-light irradiation but it becomes lower under ultraviolet (UV)-irradiation. Herein, pure rutile TiO_2, pure anatase TiO_2, and TiO_2 of hybrid phases with and without GQDs sensitization were fabricated into photoanodes to measure their photoelectrical properties. The mechanism of the photon-generated photocurrent in pure TiO_2 nanofibers may be mainly ascribed to two aspects: (i) electrons are excited from the valence band to conduction band by absorbing photons with higher energy than the band gap (Scheme 3, red lines); (ii) electrons are excited from the valence band to surface states with photons of much lower energy (Scheme 3, green lines). Jing et al.[32] attributed this weak optical absorption of nanostructured TiO_2 under the irradiation between 400 and 550 nm to the existence of surface states: impurities and defects such as oxygen vacancies[33] in nanostructured TiO_2 lead to those subbands (Scheme 3, dotted lines), which are always located between the valence band and conduction band. As a result, photons with lower energy than the band gap are able to achieve the surface state transition instead of the band-to-band transition that requires photons with much higher energy. This could also explain the tiny PL property of pure TiO_2 we have discussed above. It is demonstrated in Fig. 2(a) (dotted lines) that the photocurrent response tremendously increases with the sintering temperature from 510 to 950 °C. This indicates that rutile TiO_2 shows higher photoelectrical activity than anatase TiO_2 since the photocurrent responses increase with more rutile TiO_2 in



SCHEME 3. A schematic illustration of various electron transition processes. Black arrows: normal PL mechanism; blue arrows: upconversion PL mechanism; red arrows: band-to-band transition of electrons in TiO_2; green arrows: surface state transition of electrons which allows the absorption of TiO_2 above 420 nm.

https://doi.org/10.1557/jmr.2014.152 Published online by Cambridge University Press

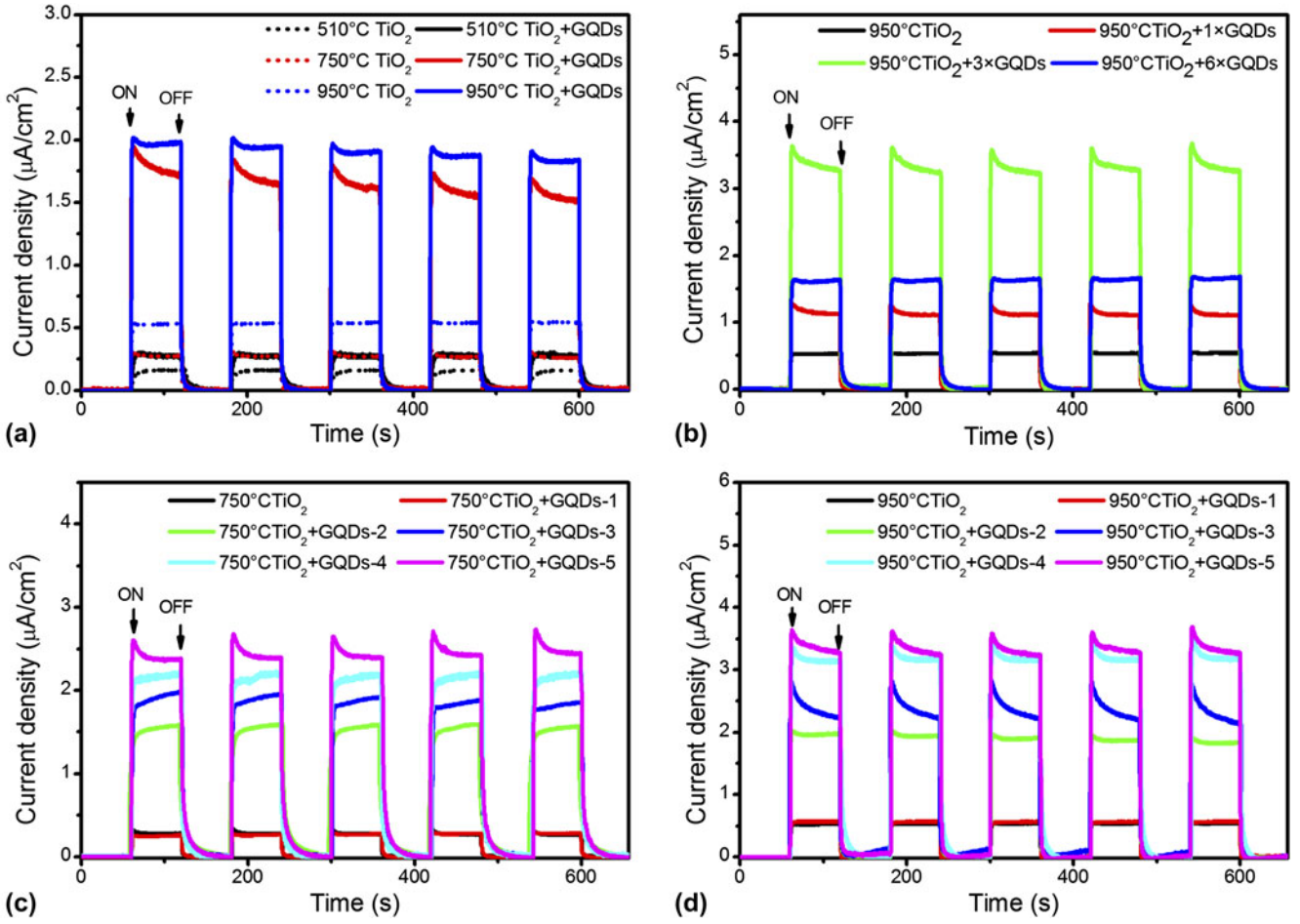


FIG. 2. Photocurrent response of GQDs-sensitized TiO_2 nanofibers. (a) Effect of the crystal morphology of TiO_2 nanofibers. (b) Effect of the GQDs' concentration. (c) and (d) Effect of the amount of N in GQDs. (1 × GQDs is the standard concentration, 3 × GQDs means three times of the 1 × GQDs.) An initial voltage of 0.2 V was imposed on the photoanodes with 420-cut (wavelength above 420 nm) irradiation of 50 mW by a Xe lamp.

the structure, probably due to the smaller band gap of rutile TiO_2. Simply, the narrower band gap of rutile TiO_2 (3.0 eV) as compared with anatase TiO_2 (3.2 eV) allows the excitation of electrons from valence band to conduction band with photons of lower energy. In this way, the total photocurrent is increased as more electrons are excited. The results achieved utilizing TiO_2 nanofibers alone agrees with previous report by Zhuo et al.[3] The TiO_2 nanofibers were subsequently sensitized by GQDs-2 and tested in the three-electrode system to obtain the excellent TiO_2 electrode for the whole device. Figure 2(a) (solid lines) shows that as compared with the lesser enhancement (~1.72 times, 0.274 μA/cm^2) of GQDs-2-sensitized TiO_2 (510 °C) nanofibers, GQDs-2-sensitized TiO_2 (750 °C) nanofibers have the highest enhancement ratio (~5.84 times, 1.56 μA/cm^2) while those of 950 °C have the highest photocurrent responses (~3.58 times, 1.91 μA/cm^2), indicating that TiO_2 nanofibers with composite crystalline phases exhibit a much higher photoelectrical activity than those of pure anatase or pure rutile TiO_2 nanofibers. This corresponds with the result of literature work.[34] The highest enhancement ratio achieved by TiO_2 nanofibers of hybrid crystalline phases (750 °C-sintered TiO_2) may be explained by their property of inhibiting the recombination of photoinduced charges, which is brought about by the electron transfer between the conduction bands of different phases. A recent study conducted by David O. Scanlon et al.[35] deeply investigated the band alignment between rutile and anatase and reached the conclusion that conduction electrons flowed from rutile to anatase. The general mechanism of the N-doped GQDs-induced photocurrent is that the narrow band gap of GQDs (~1.15 eV for GQDs-5, calculated by cyclic voltammetry (Fig. S7)) makes it possible to excite electrons from highest occupied molecular orbital (HOMO) to lowest unoccupied molecular orbital (LUMO), which transfer to the conduction band of TiO_2 followed by the transition to the surface of FTO. In this way, photons with much higher wavelengths can be absorbed to generate photoinduced electrons which extensively increase the total value of photocurrent. The extent of aggregation, which depends on the fabrication of the devices and the concentration of the GQDs suspension, was also found to deeply

https://doi.org/10.1557/jmr.2014.152 Published online by Cambridge University Press

influence the photoelectric properties. It has been found that graphene-based materials have the tendency to form aggregates in suspension related with strong van der Waals interactions and hydrogen bonds.[36] Aggregation is observed to cause both rough film morphology and incomplete film coverage on the glass surface, which may heavily inhibit the formation and conveying of electron/hole pairs and limit their photoelectrical application. This result agrees with previous findings by Zhang et al.[37] that this kind of agglomeration heavily decreases the contact area of the two adhered materials thus leads to the inevitable reduction of the photoelectrical property. Herein, we choose not to mix GQDs with the TiO_2 suspension but to use the so-called "layer-by-layer" method to prepare the composite structure, which avoids the direct suspension–suspension interaction. Measures should be taken to prepare the composite structure with acceptable extent of aggregation that may not exert a fatal influence on the generation and transportation of electron/hole pairs. After a series of experiments, we found that in spite of experimental skills, the concentration of GQDs suspension played a decisive role on the quality of the films. The level of aggregation evidently increased with the augmented GQDs concentration. Nevertheless, we faced a dilemma that when the concentration was reduced, it led to the degradation of the sensitization effect of TiO_2 nanofibers and also impaired the photoelectrical property of the composite structure. Figure 2(b) demonstrates that a balanced concentration of the GQDs should be used, based on the two decisive parameters above. The concentration of 3× (three times of the standard concentration) appears to harvest the best effect in terms of the enhancement of photocurrent response and thus GQDs suspension of 3x concentration was used in all the later experiments. Visible aggregation leads to the decrease of photocurrent response if the concentration reaches 6x concentration. The N amount in GQDs is another important factor that affects the degree of sensitization. N-doped GQDs exhibit some varying characteristics as compared with N-free ones according to literature work.[13] As compared with the nonenhancement of the photocurrent response of N-free GQDs-1, N-doped GQDs (GQDs-2, 3, 4, 5) exhibit substantial improvement which increases with the increasing N concentration [Figs. 2(c) and 2(d)] due to their distinctive PL property and n-type behavior toward the Ti semiconductor. Their changed PL property as compared with N-free GQDs is primarily demonstrated by the fact that the intensity of PL peaks rises with the increasing amount of ammonia in GQDs (see Fig. S8), which means more electrons can be excited to generate photocurrents. A blue shift of approximately 20 nm was also found in N-doped GQDs in comparison with the N-free ones. The absorption of photons with higher energy may also add to the generated photocurrents. Li et al. proposed that the relatively strong electron affinity of N in N-GQDs might result in the blue shift of PL peaks.[38] Furthermore, N-doped graphene-related materials like N-doped graphene[39] and N-doped graphene nanoribbons[40] always exhibit n-type conductivity as a result of nitrogen present in the π-conjugated system or its electrons-donating property toward the π system. Therefore, we propose that the graphene-derived N-doped GQDs also show n-type behavior which exerts significant influence on the electrical conductivity of the semiconductor. In a word, after considering several parameters including the crystalline phase of the TiO_2 electrode, the concentration of GQDs suspension used to sensitize, and the N amount in GQDs, we find that the N-doped GQDs (3x concentration) sensitized 750 °C-sintered TiO_2 (mixed phases) nanofibers exhibit the best enhancement in the photoelectrical property and the enhancement increases with more N doped in GQDs.

To further investigate the electron generation and transfer mechanism of GQDs-sensitized TiO_2 nanofibers, the effect of irradiation wavelength on photocurrent responses was studied using 750 °C-sintered TiO_2 nanofibers as the electrode material (Figs. 3 and 4). Evident enhancement of photocurrent response can be detected at the wavelength of 420, 450, 475, and 550 nm after sensitization (Fig. 4). Specially, nonenhancement of N-free GQDs-1 and the increasing enhancement with more N added are corresponded with the result in Figs. 2(c) and 2(d). Since graphene-based materials have long been used in composite with TiO_2 to enhance the photoelectrical property, previous studies explored the irradiation-wavelength-dependent property of graphene-based TiO_2 composites. For instance, RGO-sensitized TiO_2 only exhibits considerable enhancement of photocurrent responses in the irradiation of above 500 nm light[17] and similarly GO/TiO_2 composites shows better photocatalytic performance than single TiO_2 under irradiation longer than 510 nm.[18] It can be found in our work that GQDs-sensitized TiO_2 nanofibers not only generate higher photocurrent above 520 nm which is similar with previous work, but also reveal tremendously improved photocurrent response between approximately 450 and 480 nm. The variation of enhancement by different wavelength irradiation can be clarified by the normal PL and upconversion PL mechanism.[13,41] To explain the phenomena, an energy level structural model (Scheme 3) was established in which the HOMO of GQDs was divided into π orbitals and σ orbitals. It is a well-known fact that the energy levels of the two orbitals are determined by the carbene ground-state multiplicity[42] and the energy difference (δE) between them should be below 1.5 eV, as shown by Hoffmann.[43] Herein, we proposed that photons below 475 nm should be absorbed following the normal PL mechanism (Scheme 3, black arrows). Namely, their energy stimulates the electrons from σ orbitals of

https://doi.org/10.1557/jmr.2014.152 Published online by Cambridge University Press

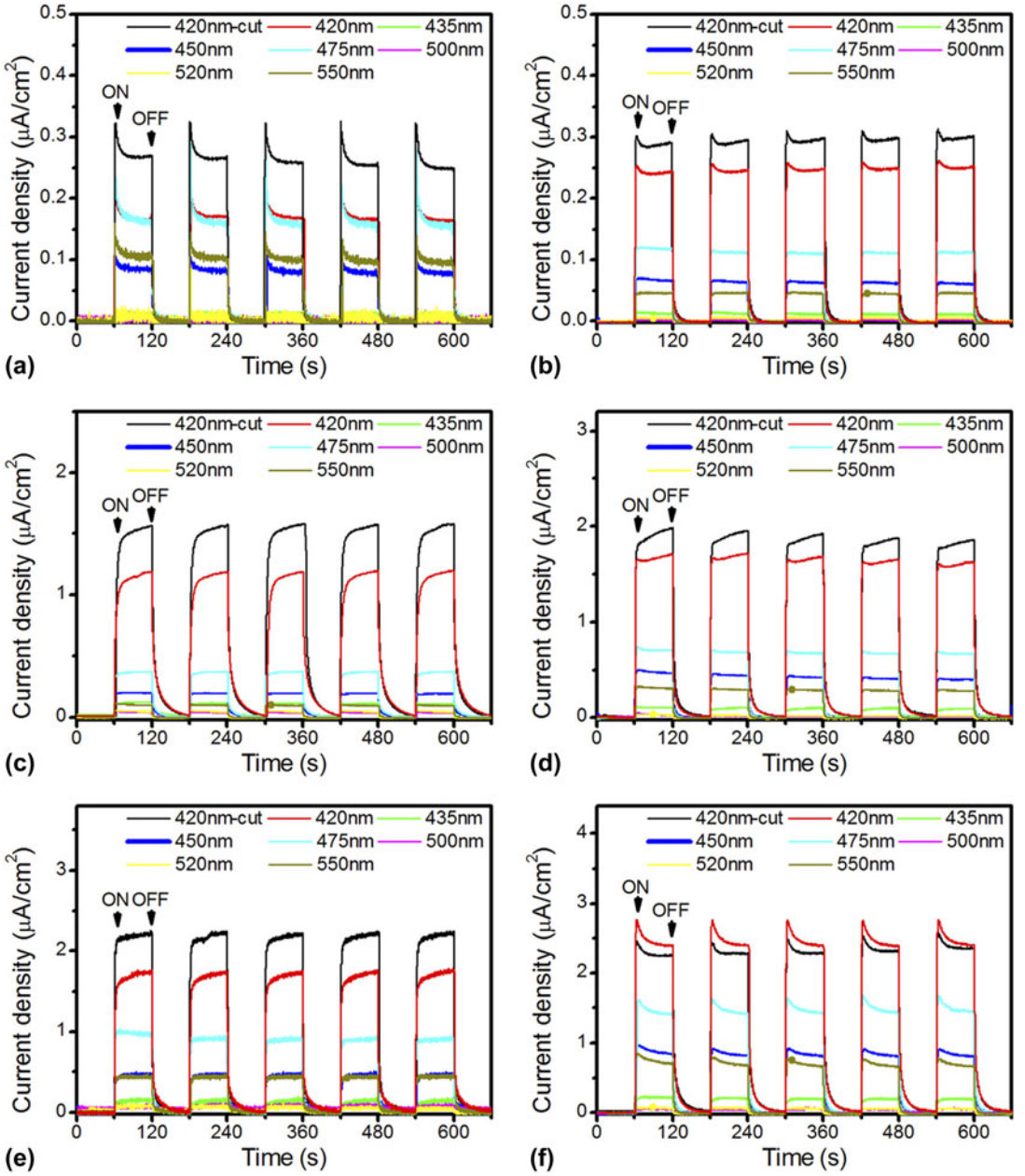


FIG. 3. Photocurrent response of (a) TiO_2 nanofibers (750 °C) and (b)–(f) GQDs-1-sensitized TiO_2 nanofibers (750 °C) to GQDs-5-sensitized TiO_2 nanofibers (750 °C) under irradiation of different wavelength.

HOMO to LUMO to start the transportation of electrons in a cycle. PL spectra of GQDs at different excitation wavelengths (Fig. S9) clearly indicate that irradiation light under approximately 460 nm exhibits apparent PL peaks which represents that photons can excite electrons in the HOMO of GQDs. This result roughly corresponded with the fact that light below 475 nm can be absorbed. By contrast, the enhancement at 550 nm irradiation may be attributed to the upconverted PL property of GQDs according to the ASPL (anti-Stokes photoluminescent) mechanism[44] (Scheme 3, blue arrows), in which the existence of π orbitals of HOMO provides a much shorter energy gap than the traditional σ orbitals of HOMO, allowing long-wavelength photons to excite electrons. Comparing with other graphene-based TiO_2 composites, GQDs-sensitized TiO_2 nanofibers undoubtedly get a superior photoelectrical property not only because they can absorb in a wider wavelength range, but also because their value of photocurrent responses is much higher (around 10 times higher than the RGO-sensitized TiO_2). Figures S10 and S11 indicate that similar results can be obtained with 950 °C-sintered TiO_2 nanofibers.

https://doi.org/10.1557/jmr.2014.152 Published online by Cambridge University Press

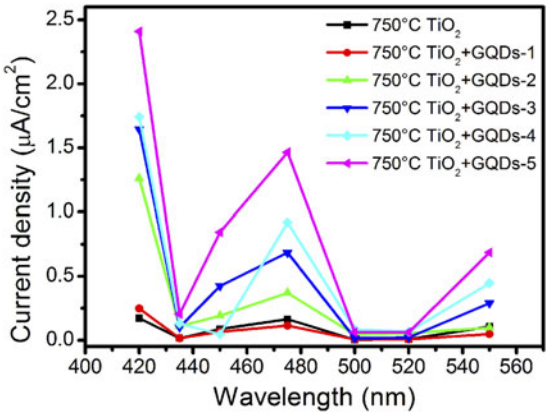


FIG. 4. Peak values of photocurrent response under irradiation of various wavelengths. All the data are normalized at irradiation intensity of 50 mW. The initial voltage imposed on photoanodes was 0.2 V.

IV. CONCLUSION

In summary, the composite structures of GQDs-sensitized TiO_2 nanofibers were prepared using a "layer-by-layer" method. TiO_2 nanofibers with anatase and rutile hybrid phases (750 °C-sintered TiO_2 nanofibers) exhibit higher photoelectrical activity than using pure rutile or pure anatase TiO_2 nanofibers as electrode material. Substantial improvement of photocurrent response was observed after the sensitization of N-doped GQDs and the enhancement increases with the increasing amount of N. This phenomenon is attributed to the enhanced PL property and n-type behavior resulting from N-doping. Especially important to the extent of sensitization and aggregation is the concentration of GQDs in suspension; as such this parameter should be precisely controlled. By controlling the wavelength of irradiation light on the three-electrode system, we find that considerable improvement of photocurrent response can only be achieved among 450–480 nm and above 520 nm range of visible light which is related to the normal PL and upconverted PL mechanisms respectively. The photocurrent generated in the GQDs-sensitized TiO_2 nanofibers system presumably results from the transfer of photoexcited electrons in GQDs to the conduction band of TiO_2 followed by their transition to the surface of FTO. The sensitization of GQDs surely enlarges the absorbance region of TiO_2 nanofibers to much longer wavelengths and extends their photovoltaic and photoelectrical application. The discovery of the improved photoelectrical performance of TiO_2 nanofibers after sensitization by N-GQDs may serve as an efficient application in photovoltaics and photocatalysis.

ACKNOWLEDGMENTS

This work was financially supported by the National Basic Research Program (973 program, 2013CB932902), the National Natural Science Foundation of China (21201034, 21173042, 2131010200, 551103023, and 21345008), the Fundamental Research Funds for the Central Universities (No. 3207044403), the Southeast University Innovation Fund (No. 3207042401) and the Science and Technology Support Program (Industry) Project of Jiangsu Province (BE 2013118).

REFERENCES

1. Ç.Ö. Girit, J.C. Meyer, R. Erni, M.D. Rossell, C. Kisielowski, L. Yang, C-H. Park, M. Crommie, M.L. Cohen, and S.G. Louie: Graphene at the edge: Stability and dynamics. *Science* **323**, 1705–1708 (2009).
2. X. Yan, X. Cui, B. Li, and L.S. Li: Large, solution-processable graphene quantum dots as light absorbers for photovoltaics. *Nano Lett.* **10**, 1869–1873 (2010).
3. S. Zhuo, M. Shao, and S-T. Lee: Upconversion and downconversion fluorescent graphene quantum dots: Ultrasonic preparation and photocatalysis. *ACS Nano* **6**, 1059–1064 (2012).
4. J. Shen, Y. Zhu, X. Yang, and C. Li: Graphene quantum dots: Emergent nanolights for bioimaging, sensors, catalysis and photovoltaic devices. *Chem. Commun.* **48**, 3686–3699 (2012).
5. L. Ponomarenko, F. Schedin, M. Katsnelson, R. Yang, E. Hill, K. Novoselov, and A. Geim: Chaotic Dirac billiard in graphene quantum dots. *Science* **320**, 356–358 (2008).
6. S.N. Baker and G.A. Baker: Luminescent carbon nanodots: Emergent nanolights. *Angew. Chem., Int. Ed.* **49**, 6726–6744 (2010).
7. S-T. Yang, L. Cao, P.G. Luo, F. Lu, X. Wang, H. Wang, M.J. Meziani, Y. Liu, G. Qi, and Y-P. Sun: Carbon dots for optical imaging in vivo. *J. Am. Chem. Soc.* **131**, 11308–11309 (2009).
8. Y. Li, Y. Hu, Y. Zhao, G. Shi, L. Deng, Y. Hou, and L. Qu: An electrochemical avenue to green-luminescent graphene quantum dots as potential electron-acceptors for photovoltaics. *Adv. Mater.* **23**, 776–780 (2011).
9. A.L.M. Reddy, A. Srivastava, S.R. Gowda, H. Gullapalli, M. Dubey, and P.M. Ajayan: Synthesis of nitrogen-doped graphene films for lithium battery application. *ACS Nano* **4**, 6337–6342 (2010).
10. H.M. Jeong, J.W. Lee, W.H. Shin, Y.J. Choi, H.J. Shin, J.K. Kang, and J.W. Choi: Nitrogen-doped graphene for high-performance ultracapacitors and the importance of nitrogen-doped sites at basal planes. *Nano Lett.* **11**, 2472–2477 (2011).
11. Y. Li, Y. Zhao, H. Cheng, Y. Hu, G. Shi, L. Dai, and L. Qu: Nitrogen-doped graphene quantum dots with oxygen-rich functional groups. *J. Am. Chem. Soc.* **134**, 15–18 (2012).
12. V.B. Parambhath, R. Nagar, and S. Ramaprabhu: Effect of nitrogen doping on hydrogen storage capacity of palladium decorated graphene. *Langmuir* **28**, 7826–7833 (2012).
13. M. Li, W. Wu, W. Ren, H-M. Cheng, N. Tang, W. Zhong, and Y. Du: Synthesis and upconversion luminescence of N-doped graphene quantum dots. *Appl. Phys. Lett.* **101**, 103107 (2012).
14. R. Liu, D. Wu, X. Feng, and K. Müllen: Bottom-up fabrication of photoluminescent graphene quantum dots with uniform morphology. *J. Am. Chem. Soc.* **133**, 15221–15223 (2011).
15. Y. Xia, P. Yang, Y. Sun, Y. Wu, B. Mayers, B. Gates, Y. Yin, F. Kim, and H. Yan: One-dimensional nanostructures: Synthesis, characterization, and applications. *Adv. Mater.* **15**, 353–389 (2003).
16. R. Long, N.J. English, and O.V. Prezhdo: Photoinduced charge separation across the graphene-TiO_2 interface is faster than energy losses: A time-domain ab initio analysis. *J. Am. Chem. Soc.* **134**, 14238–14248 (2012).
17. A. Du, Y.H. Ng, N.J. Bell, Z. Zhu, R. Amal, and S.C. Smith: Hybrid graphene/titania nanocomposite: Interface charge transfer, hole doping, and sensitization for visible light response. *J. Phys. Chem. Lett.* **2**, 894–899 (2011).

https://doi.org/10.1557/jmr.2014.152 Published online by Cambridge University Press

18. C. Chen, W. Cai, M. Long, B. Zhou, Y. Wu, D. Wu, and Y. Feng: Synthesis of visible-light responsive graphene oxide/TiO_2 composites with p/n heterojunction. *ACS Nano* **4**, 6425–6432 (2010).
19. Y. Dai, Y. Sun, J. Yao, D. Ling, Y. Wang, H. Long, X. Wang, B. Lin, T.H. Zeng, and Y. Sun: Graphene-wrapped TiO_2 nanofibers with effective interfacial coupling as ultrafast electron transfer bridges in novel photoanodes. *J. Mater. Chem. A* **2**, 1060–1067 (2014).
20. W. Shockley and H.J. Queisser: Detailed balance limit of efficiency of p-n junction solar cells. *J. Appl. Phys.* **32**, 510–519 (1961).
21. K.J. Williams, C.A. Nelson, X. Yan, L-S. Li, and X. Zhu: Hot electron injection from graphene quantum dots to TiO_2. *ACS Nano* **7**, 1388–1394 (2013).
22. Y. Dai, Y. Jing, J. Zeng, Q. Qi, C. Wang, D. Goldfeld, C. Xu, Y. Zheng, and Y. Sun: Nanocables composed of anatase nanofibers wrapped in UV-light reduced graphene oxide and their enhancement of photoinduced electron transfer in photoanodes. *J. Mater. Chem.* **21**, 18174–18179 (2011).
23. Y. Dai, H. Long, X. Wang, Y. Wang, Q. Gu, W. Jiang, Y. Wang, C. Li, T.H. Zeng, and Y. Sun: Versatile graphene quantum dots with tunable nitrogen doping. *Part. Part. Syst. Charact.* **31**, 597–604 (2013).
24. W.S. Hummers, Jr., and R.E. Offeman: Preparation of graphitic oxide. *J. Am. Chem. Soc.* **80**, 1339 (1958).
25. W. Zhang, M. Zhang, Z. Yin, and Q. Chen: Photoluminescence in anatase titanium dioxide nanocrystals. *Appl. Phys. B* **70**, 261–265 (2000).
26. Z. Lide and C-M. Mo: Luminescence in nanostructured materials. *Nanostruct. Mater.* **6**, 831–834 (1995).
27. J. Shen, B. Yan, M. Shi, H. Ma, N. Li, and M. Ye: One step hydrothermal synthesis of TiO_2-reduced graphene oxide sheets. *J. Mater. Chem.* **21**, 3415–3421 (2011).
28. D. Luo, G. Zhang, J. Liu, and X. Sun: Evaluation criteria for reduced graphene oxide. *J. Phys. Chem. C* **115**, 11327–11335 (2011).
29. K.N. Kudin, B. Ozbas, H.C. Schniepp, R.K. Prud'Homme, I.A. Aksay, and R. Car: Raman spectra of graphite oxide and functionalized graphene sheets. *Nano Lett.* **8**, 36–41 (2008).
30. Y-H. Zhang, C.K. Chan, J.F. Porter, and W. Guo: Micro-Raman spectroscopic characterization of nanosized TiO_2 powders prepared by vapor hydrolysis. *J. Mater. Res.* **13**, 2602–2609 (1998).
31. Q. Yang, C. Xie, Z. Xu, Z. Gao, and Y. Du: Synthesis of highly active sulfate-promoted rutile titania nanoparticles with a response to visible light. *J. Phys. Chem. B* **109**, 5554–5560 (2005).
32. L. Jing, S. Li, S. Song, L. Xue, and H. Fu: Investigation on the electron transfer between anatase and rutile in nano-sized TiO_2 by means of surface photovoltage technique and its effects on the photocatalytic activity. *Sol. Energy Mater. Sol. Cells* **92**, 1030–1036 (2008).
33. Y. Zhang, G. Li, Y. Jin, Y. Zhang, J. Zhang, and L. Zhang: Hydrothermal synthesis and photoluminescence of TiO_2 nanowires. *Chem. Phys. Lett.* **365**, 300–304 (2002).
34. M.S.P. Francisco and V.R. Mastelaro: Inhibition of the anatase-rutile phase transformation with addition of CeO_2 to CuO-TiO_2 system: Raman spectroscopy, x-ray diffraction, and textural studies. *Chem. Mater.* **14**, 2514–2518 (2002).
35. D.O. Scanlon, C.W. Dunnill, J. Buckeridge, S.A. Shevlin, A.J. Logsdail, S.M. Woodley, C.R.A. Catlow, M.J. Powell, R.G. Palgrave, and I.P. Parkin: Band alignment of rutile and anatase TiO_2. *Nat. Mater.* **12**, 798–801 (2013).
36. S. Morales-Torres, L.M. Pastrana-Martinez, J.L. Figueiredo, J.L. Faria, and A.M. Silva: Design of graphene-based TiO_2 photocatalysts – A review. *Environ. Sci. Pollut. Res. Int.* **19**, 3676–3687 (2012).
37. Q. Zhang, Y. He, X. Chen, D. Hu, L. Li, T. Yin, and L. Ji: Structure and photocatalytic properties of TiO_2-graphene oxide intercalated composite. *Chin. Sci. Bull.* **56**, 331–339 (2011).
38. Q. Li, S. Zhang, L. Dai, and L.S. Li: Nitrogen-doped colloidal graphene quantum dots and their size-dependent electrocatalytic activity for the oxygen reduction reaction. *J. Am. Chem. Soc.* **134**, 18932–18935 (2012).
39. D. Wei, Y. Liu, Y. Wang, H. Zhang, L. Huang, and G. Yu: Synthesis of N-doped graphene by chemical vapor deposition and its electrical properties. *Nano Lett.* **9**, 1752–1758 (2009).
40. Y. Li, Z. Zhou, P. Shen, and Z. Chen: Spin gapless semiconductor-metal-half-metal properties in nitrogen-doped zigzag graphene nanoribbons. *ACS Nano* **3**, 1952–1958 (2009).
41. J. Shen, Y. Zhu, C. Chen, X. Yang, and C. Li: Facile preparation and upconversion luminescence of graphene quantum dots. *Chem. Commun.* **47**, 2580–2582 (2011).
42. D. Pan, J. Zhang, Z. Li, C. Wu, X. Yan, and M. Wu: Observation of pH-, solvent-, spin-, and excitation-dependent blue photoluminescence from carbon nanoparticles. *Chem. Commun.* **46**, 3681–3683 (2010).
43. R. Hoffmann: Trimethylene and the addition of methylene to ethylene. *J. Am. Chem. Soc.* **90**, 1475–1485 (1968).
44. X. Wang, W.W. Yu, J. Zhang, J. Aldana, X. Peng, and M. Xiao: Photoluminescence upconversion in colloidal CdTe quantum dots. *Phys. Rev. B* **68**, 125318 (2003).

https://doi.org/10.1557/jmr.2014.152 Published online by Cambridge University Press